Research Article | Vol. 25, No. 4 | 20 Feb 2017 | OPTICS EXPRESS 3252

Optics EXPRESS

Wavelength conversion of complex modulation formats in a compact SiGe waveguide

M. A. ETTABIB,[1,*] C. LACAVA,[1] Z. LIU,[1] A. BOGRIS,[2,3] A. KAPSALIS,[2] M. BRUN,[4] P. LABEYE,[4] S. NICOLETTI,[4] D. SYVRIDIS,[2] D. J. RICHARDSON [1] AND P. PETROPOULOS[1]

[1]*Optoelectronics Research Centre, University of Southampton, Southampton, SO17 1BJ, UK,*
[2]*Department of Informatics and Telecommunications, National and Kapodistrian University of Athens, Panepistimiopolis, Ilissia, 15784, Athens, Greece*
[3]*Department of Informatics, Technological Educational institute of Athens, Egaleo, Athens, Greece*
[4]*CEA-Leti MINATEC Campus, 17 rue des Martyrs 38054 Grenoble Cedex 9, France*
[*]*mae206@orc.soton.ac.uk*

Abstract: We report a nonlinear signal processing system based on a SiGe waveguide suitable for high spectral efficiency data signals. Four-wave-mixing (FWM)-based wavelength conversion of 10-Gbaud 16-Quadrature amplitude modulated (QAM) and 64-QAM signals is demonstrated with less than −10-dB conversion efficiency (CE), 36-dB idler optical signal-to-noise ratio (OSNR), negligible bit error ratio (BER) penalty and a 3-dB conversion bandwidth exceeding 30nm. The SiGe device was CW-pumped and operated in a passive scheme without giving rise to any two-photon absorption (TPA) effects.

OCIS codes: (130.7405) Wavelength conversion devices; (190.4390) Nonlinear optics, integrated optics; (190.4380) Nonlinear optics, four-wave mixing; (230.7390) Waveguides, planar.

References and links

1. D. J. Richardson, "Applied physics. Filling the light pipe," Science **330**(6002), 327–328 (2010).
2. T. Kobayashi, A. Sano, A. Matsuura, Y. Miyamoto, and K. Ishihara, "Nonlinear tolerant spectrally-efficient transmission using PDM 64-QAM single carrier FDM with digital pilot-tone," J. Lightwave Technol. **30**(24), 3805–3815 (2012).
3. R. Adams, M. Spasojevic, M. Chagnon, M. Malekiha, J. Li, D. V. Plant, and L. R. Chen, "Wavelength conversion of 28 GBaud 16-QAM signals based on four-wave mixing in a silicon nanowire," Opt. Express **22**(4), 4083–4090 (2014).
4. C. Li, C. Gui, X. Xiao, Q. Yang, S. Yu, and J. Wang, "On-chip all-optical wavelength conversion of multicarrier, multilevel modulation (OFDM m-QAM) signals using a silicon waveguide," Opt. Lett. **39**(15), 4583–4586 (2014).
5. Y. Long, J. Liu, X. Hu, A. Wang, L. Zhou, K. Zou, Y. Zhu, F. Zhang, and J. Wang, "All-optical multi-channel wavelength conversion of Nyquist 16 QAM signal using a silicon waveguide," Opt. Lett. **40**(23), 5475–5478 (2015).
6. F. P. Guiomar, S. B. Amado, A. Carena, G. Bosco, A. Nespola, A. L. Teixeira, and A. N. Pinto, "Fully blind linear and nonlinear equalization for 100G PM-64QAM optical systems," J. Lightwave Technol. **33**(7), 1265–1274 (2015).
7. R. Slavík, A. Bogris, F. Parmigiani, J. Kakande, M. Westlund, M. Sköld, L. Grüner-Nielsen, R. Phelan, D. Syvridis, P. Petropoulos, and D. J. Richardson, "Coherent all-optical phase and amplitude regenerator of binary phase-encoded signals," IEEE J. Sel. Top. Quantum Electron. **18**(2), 859–869 (2012).
8. M. Dinu, F. Quochi, and H. Garcia, "Third-order nonlinearities in silicon at telecom wavelengths," Appl. Phys. Lett. **82**(18), 2954–2956 (2003).
9. C. Koos, P. Vorreau, T. Vallaitis, P. Dumon, W. Bogaerts, R. Baets, B. Esembeson, I. Biaggio, T. Michinobu, F. Diederich, W. Freude, and J. Leuthold, "All-optical high-speed signal processing with silicon – organic hybrid slot waveguides," Nat. Photonics **3**(4), 216 (2009).
10. A. Trita, C. Lacava, P. Minzioni, J. P. Colonna, P. Gautier, J. M. Fedeli, and I. Cristiani, "Ultra-high four wave mixing efficiency in slot waveguides with silicon nanocrystals," Appl. Phys. Lett. **99**(19), 191105 (2011).
11. M. A. Ettabib, A. Kapsalis, A. Bogris, F. Parmigiani, V. J. F. Rancano, K. Bottrill, M. Brun, P. Labeye, S. Nicoletti, K. Hammani, D. Syvridis, D. J. Richardson, and P. Petropoulos, "Polarization Insensitive Wavelength Conversion in a Low-Birefringence SiGe Waveguide," IEEE Photonics Technol. Lett. **28**(11), 1221–1224 (2016).

#281549 https://doi.org/10.1364/OE.25.003252
Journal © 2017 Received 24 Nov 2016; revised 20 Jan 2017; accepted 25 Jan 2017; published 7 Feb 2017

Optics EXPRESS

12. C. Lacava, M. A. Ettabib, I. Cristiani, J. M. Fedeli, D. J. Richardson, and P. Petropoulos, "Ultra-Compact Amorphous Silicon Waveguide for Wavelength Conversion," IEEE Photonics Technol. Lett. **28**(4), 410–413 (2016).
13. M. Ettabib, K. Bottrill, F. Parmigiani, A. Kapsalis, A. Bogris, M. Brun, P. Labeye, S. Nicoletti, K. Hammani, D. Syvridis, D. J. Richardson, and P. Petropoulos, "All-optical Phase Regeneration with Record PSA Extinction Ratio in a Low-birefringence Silicon Germanium Waveguide," J. Lightwave Technol. **34**(17), 3993–3998 (2016).
14. F. Da Ros, D. Vukovic, A. Gajda, K. Dalgaard, L. Zimmermann, B. Tillack, M. Galili, K. Petermann, and C. Peucheret, "Phase regeneration of DPSK signals in a silicon waveguide with reverse-biased p-i-n junction," Opt. Express **22**(5), 5029–5036 (2014).
15. K. Hammani, M. A. Ettabib, A. Bogris, A. Kapsalis, D. Syvridis, M. Brun, P. Labeye, S. Nicoletti, D. J. Richardson, and P. Petropoulos, "Optical properties of silicon germanium waveguides at telecommunication wavelengths," Opt. Express **21**(14), 16690–16701 (2013).
16. K. Hammani, M. A. Ettabib, A. Bogris, A. Kapsalis, D. Syvridis, M. Brun, P. Labeye, S. Nicoletti, and P. Petropoulos, "Towards nonlinear conversion from mid- to near-infrared wavelengths using Silicon Germanium waveguides," Opt. Express **22**(8), 9667–9674 (2014).
17. M. A. Ettabib, L. Xu, A. Bogris, A. Kapsalis, M. Belal, E. Lorent, P. Labeye, S. Nicoletti, K. Hammani, D. Syvridis, D. P. Shepherd, J. H. V. Price, D. J. Richardson, and P. Petropoulos, "Broadband telecom to mid-infrared supercontinuum generation in a dispersion-engineered silicon germanium waveguide," Opt. Lett. **40**(17), 4118–4121 (2015).

1. Introduction

Optical communication networks have recently witnessed a sustained growth in traffic, driven by an increasing number of network users and the rapid adoption of high bandwidth applications [1]. This has led researchers to investigate approaches to cope with this increased demand for bandwidth, through e.g. the use of complex modulation formats that lead to a more efficient use of the available bandwidth. Quadrature amplitude modulation (QAM) formats, such as 16-QAM and 64-QAM, have received increasing interest recently [2–5], since they allow for a more efficient use of the optical spectrum than the more widely adopted formats of on-off keying (OOK), differential phase-shift keying (DPSK) and quadrature phase-shift keying (QPSK). However, the transmission and processing of QAM signals present a significant challenge. QAM signals are susceptible to both linear and nonlinear phase noise, and require high optical signal to noise ratios (OSNRs) in reception [6,7]. Therefore, the performance requirements on processing systems (such as wavelength converters (WCs) and phase conjugators) designed for such signals are much more stringent than in simpler modulation formats.

Nonlinear silicon devices have recently emerged as promising candidates for implementing all-optical signal processing functions due to the ultra-high $\chi^{(3)}$ nonlinearity of silicon and their potential for realizing nonlinear devices with small footprint, high yield and low fabrication costs [8,9]. Indeed, several important applications, including wavelength conversion [3,10–12] and optical regeneration [13,14] have already been demonstrated in systems based on either crystalline silicon, amorphous silicon or silicon germanium.

Silicon germanium in particular, presents itself as a promising and versatile platform for all-optical processing applications in the near-IR [13,15]. This is due to the facility of tailoring the optical properties of SiGe waveguides, including the Kerr response and the TPA threshold, through control of the Ge doping concentration and profile [15]. In this paper, we exploit these attributes in a new SiGe nonlinear waveguide design that adopts a gradient Ge concentration and an air-clad structure, and incorporates an efficient taper for light-coupling. These design features have resulted in waveguides with a threefold increase in the nonlinearity and 3.5dB improvement in coupling efficiency relative to earlier results on the same material platform [11,13]. We use these devices to demonstrate wavelength conversion of complex modulation formats. We report FWM-based wavelength conversion of 10 Gbaud 16-QAM and 64-QAM signals in a 10mm-long SiGe device using CW pumping and requiring no active TPA suppression. We demonstrate a conversion efficiency of –9.7 dB and generate an idler with an OSNR as high as 36 dB. A negligible BER conversion penalty is

Optics EXPRESS

achieved. The 64-QAM wavelength conversion represents the most complex single-channel modulation format ever processed in a silicon-based device.

2. Device description

Figure 1 (left) illustrates the geometrical design of the SiGe device, which was a strip air-clad waveguide with a width of 0.6µm and a height of 1.6µm. The device was grown by reduced-pressure chemical vapour deposition (RPCVD) on a silicon-on-insulator (SOI) wafer with a 2-µm buried oxide layer (BOX) and an upper silicon layer thickness of 400nm. An epitaxial growth of 300nm-thick silicon was made in order to implement a 700nm silicon layer between the BOX and the SiGe waveguide core. The SiGe graded index core was then also epitaxially grown on top of the silicon layer. The waveguide was then realized by photolithography and SiGe reactive ion etching. Figure 1 (right) shows a waveguide sample image of a waveguide with a nominal width of 0.5µm. A small over-etch is perceptible, however, we have not experienced any device performance degradation because of it.

An issue compromising the practicality of compact silicon-based devices is the poor coupling efficiency from fiber systems. In order to address this, large tapered waveguides were realized at the input and output interfaces and were combined with an upper silicon cladding taper (to reduce the numerical aperture). As it is extremely difficult to realize a top silicon taper by photolithography and etching above the waveguide, it was decided to use silicon epitaxy in a silica stamp (itself realized by photolithography and etching). Figure 2 shows this realization principle. On the left is the structure after the silica stamp realization and before silicon epitaxial growth. In the middle, the structure after silicon epitaxial growth is shown and on the right, the final taper above the waveguide after chemical mechanical polishing and SiO_2 etching.

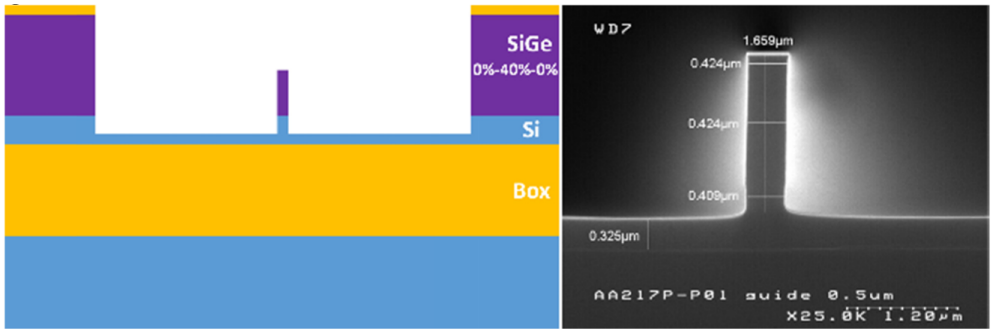

Fig. 1. A schematic of the device structure (left) and scanning electron microscopy (SEM) image of the waveguide.

Light coupling into the waveguide was achieved using a commercial lensed fiber with a spot size of 2 µm, resulting in an overall coupling loss of ~4.5 dB. Experimental characterization of the TE mode of the fabricated waveguide revealed that it exhibited losses close to 6 dB/cm at 1.55 µm. The nonlinear coefficient $\mathrm{Re}\{\gamma\}$ of the waveguide was also measured at the same wavelength using the dual-frequency beat signal method [15] and found to be 67 /W/m, which is in close agreement with the numerically simulated value of 70 /W/m.

Optics EXPRESS

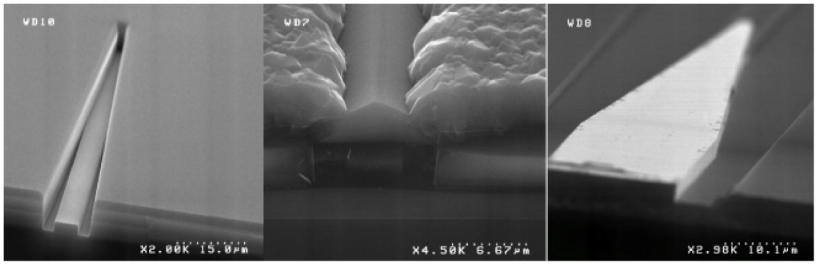

Fig. 2. Taper realization steps.

The waveguide has been designed so as to permit enhanced nonlinear interaction for a wide range of wavelengths. Numerical simulation of the dispersion of the waveguide predict a dispersion of – 480 ps/nm/km at 1550 nm. In terms of modal properties, the waveguide exhibits multi-mode behavior in the telecom band. Despite this fact, the taper filter at the input of the waveguide and the high quality in terms of roughness and shape do not allow for the generation of higher-order modes at 1550 nm.

3. Experimental setup and results

Figure 3 shows the experimental setup of the FWM-based wavelength converter (WC). The data signals were generated at a symbol rate of 10 Gbaud using a two-channel arbitrary waveform generator (AWG, Tektronix AWG7122C) operating at a sampling rate of 10 GSa/s and with 10 bits resolution. A tuneable CW laser was modulated with the data and was combined with a CW pump laser operating at 1557.64 nm using a 50/50 coupler. The combined pump and data signals were subsequently amplified using an EDFA and coupled into the SiGe waveguide. The improved coupler design as well as the high TPA and damage threshold of the device [15] allowed a power level of 28.5 dBm to be coupled into the waveguide without requiring any active TPA suppression or damaging the device. At the output, the generated idler was filtered using a tuneable bandpass filter and sent to an optically pre-amplified coherent receiver followed by a 4-channel 16 GHz, 40 GSa/s real-time scope to assess the performance of the wavelength converter in terms of bit-error ratio (BER) measurements and constellation analysis.

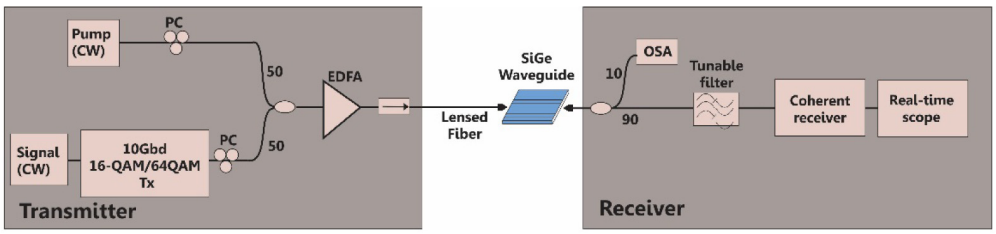

Fig. 3. The experimental setup of the FWM-based wavelength converter.

Figure 4 shows a typical optical spectrum measured at the output of the waveguide. The figure shows that for the input power used, a FWM conversion efficiency (CE- defined as the ratio of the power of the converted idler to the output signal power) of –9.7 dB was obtained. This allowed an idler with an OSNR of 36 dB (Res = 0.1nm) to be generated.

In separate experiments, the bandwidth of the wavelength converter was also characterized within the C-band. In order to study the conversion bandwidth across as much of the gain band of our EDFA (~30 nm), we shifted the wavelength of the pump source to edge of the gain band (1564.39nm) for these measurements, and varied the signal wavelength between 1548.39nm and 1564nm. Figure 5 plots the corresponding variation in FWM

Optics EXPRESS

conversion efficiency as a function of pump-signal detuning. As can be seen, the CE exhibits an almost uniform profile with less than 0.5 dB variation across the wavelengths scanned.

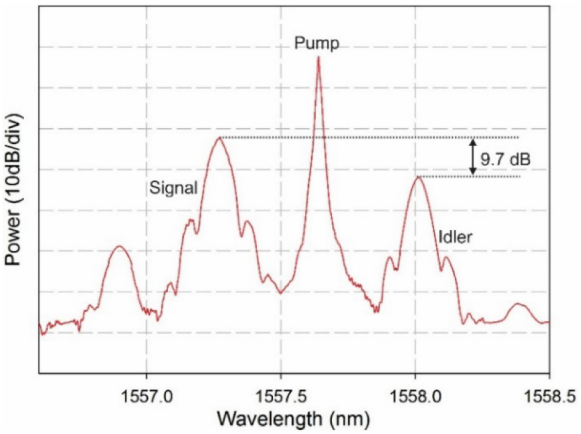

Fig. 4. Output optical spectrum of the wavelength converter.

Data signal experiments were carried out first on the 16-QAM modulation format (according to the signal-pump wavelength assignment displayed in Fig. 4). The insets to Fig. 6 display constellation diagrams of the original data signal (B2B) (left) and the idler (right). The B2B measurement exhibited a root-mean-square (rms) error vector magnitude (EVM) of 8.6%, while the corresponding measurement for the idler was 8.7%. This demonstrates that the wavelength converter results in almost no loss in quality in the converted signal (idler) in comparison to the original B2B signal. BER measurements were collected for both the B2B signal and the idler. Figure 6 shows that a negligible BER penalty (less than 0.3 dB at a BER of 10^{-3}) was obtained as a result of the conversion, confirming the observations from the EVM measurements.

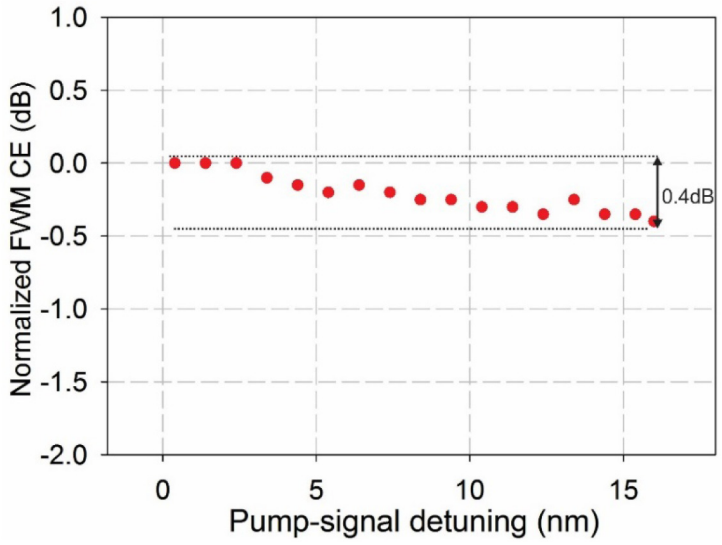

Fig. 5. Normalized FWM conversion efficiency (dB) as a function of pump-signal detuning (nm).

Optics EXPRESS

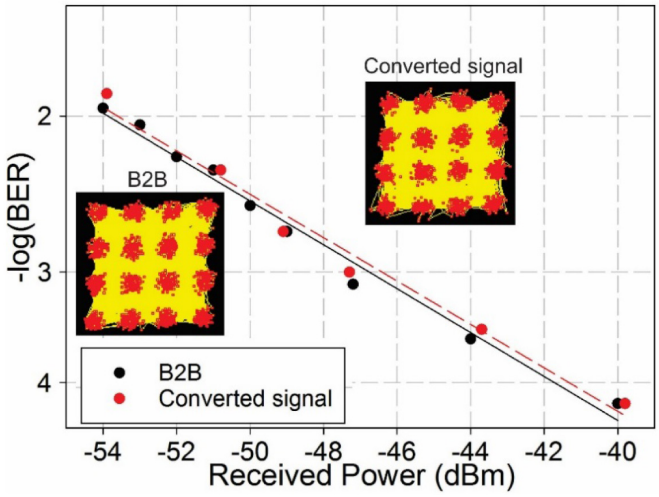

Fig. 6. BER curves and constellation diagrams for the 16-QAM B2B and the idler signals.

Previously published research has demonstrated wavelength conversion of single channel 16-QAM signals (at 28Gbaud) in a dispersion engineered silicon nanowire [3]. Multi-carrier orthogonal frequency-division multiplexed (OFDM) m-QAM signals have also been successfully wavelength-converted (at 3.2 Gbaud) in a silicon-on-insulator nanowire [4]. The results presented herein, represent a significant improvement in the performance in terms of conversion efficiency, idler OSNR, BER penalty and allowable pump power (while keeping the device operation below the TPA threshold). To further highlight the performance of the WC in processing complex, high spectral efficiency data signals, a 10 Gbaud 64-QAM signal was wavelength-converted next. In this case, offline processing was performed for signal demodulation and BER calculation. The insets to Fig. 7 display the constellation diagrams of both the original 64-QAM data signal (B2B) and the idler. The figure shows a small degradation in the quality of the idler as a result of the conversion. The rms EVM figure of both the B2B and idler were similar, with 15.5% measured for the B2B and 15.8% for the idler.

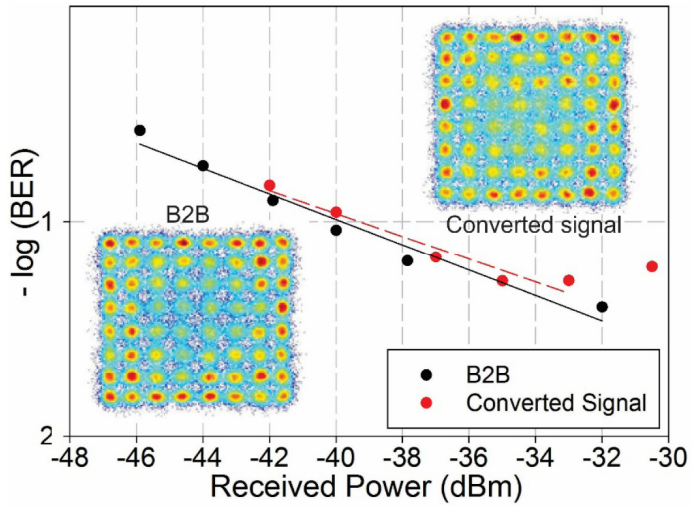

Fig. 7. BER curves and constellation diagrams for the 64-QAM B2B and the idler signals.

Optics EXPRESS

The BER curves of the 64-QAM B2B signal and idler are shown in Fig. 7. The BER of the 64-QAM signal (5.9×10^{-2}) was limited by the bandwidth (9.6 GHz at –20 dB) and effective number of bits of our AWG. However, for the sole purpose of contrasting the quality of the B2B and converted signal (and hence the performance of the wavelength converter), it can be seen that the two BER curves are similar with an error floor developing on the converted signal at high values of received power.

4. Conclusion

We have reported the performance of a highly nonlinear SiGe waveguide when used for FWM-based processing of advanced modulation formats. Wavelength conversion of 10 Gbaud 16-QAM and 64-QAM signals was demonstrated in a 10-mm long passive SiGe waveguide using CW pumping conditions, achieving a constant conversion efficiency of –9.7 dB over a 30nm wavelength span. The efficient wavelength conversion process enabled the generation of an idler with a high OSNR, resulting in a negligible BER conversion penalty for both the 16- and 64-QAM demonstrations. These results, along with previous demonstrations [11,13], highlight the versatility of the SiGe waveguide platform and its strong potential in implementing a wide range of state-of-the-art all-optical signal processing applications both in the near- and the mid-infrared [16,17]. The data for this paper can be found at DOI: 10.5258/SOTON/405173.

Funding

This work was supported by the European Communities Seventh Frame-work Programme FP7/2007-2013 under Grant 288304 (STREP CLARITY) and the Photonics Hyperhighway Programme Grant (EPSRC grant EP/I01196X).